JOURNAL OF ENVIRONMENTAL SCIENCES 127 (2023) 336–348

Available online at www.sciencedirect.com

ScienceDirect

www.elsevier.com/locate/jes

JES JOURNAL OF ENVIRONMENTAL SCIENCES

www.jesc.ac.cn

Transgenerational bone toxicity in F3 medaka (*Oryzias latipes*) induced by ancestral benzo[a]pyrene exposure: Cellular and transcriptomic insights

Jiezhang Mo[1,2,3,**], *Miles Teng Wan*[3,**], *Doris Wai-Ting Au*[2,3,***], *Jingchun Shi*[3], *Nathan Tam*[3], *Xian Qin*[3], *Napo K.M. Cheung*[3], *Keng Po Lai*[3,4], *Christoph Winkler*[5], *Richard Yuen-Chong Kong*[1,2,3,*], *Frauke Seemann*[1,6,*]

[1] *Southern Marine Science and Engineering Guangdong Laboratory (Guangzhou), Guangzhou 510000, China*
[2] *Shenzhen Key Laboratory for the Sustainable Use of Marine Biodiversity, Research Centre for the Oceans and Human Health, Shenzhen Research Institute, City University of Hong Kong, Shenzhen 518057, China*
[3] *State Key Laboratory of Marine Pollution and Department of Chemistry, City University of Hong Kong, Hong Kong SAR, China*
[4] *Laboratory of Environmental Pollution and Integrative Omics, Guilin Medical University, Huan Cheng North 2nd Road 109, Guilin 541004, China*
[5] *Department of Biological Sciences, National University of Singapore, 119077, Singapore*
[6] *Center for Coastal Studies and Department of Life Sciences, Texas A&M University-Corpus Christi, Corpus Christi, Texas 78412, USA*

ARTICLE INFO

Article history:
Received 21 February 2022
Revised 28 April 2022
Accepted 29 April 2022
Available online 10 May 2022

Keywords:
Polycyclic aromatic hydrocarbons (PAHs)
Transcriptome
Impaired bone formation
Molecular pathways
MicroRNAs
Medaka (*Oryzias latipes*)

ABSTRACT

Benzo[a]pyrene (BaP), a ubiquitous pollutant, raises environmental health concerns due to induction of bone toxicity in the unexposed offspring. Exposure of F0 ancestor medaka (*Oryzias latipes*) to 1 μg/L BaP for 21 days causes reduced vertebral bone thickness in the unexposed F3 male offspring. To reveal the inherited modifications, osteoblast (OB) abundance and molecular signaling pathways of transgenerational BaP-induced bone thinning were assessed. Histomorphometric analysis showed a reduction in OB abundance. Analyses of the miRNA and mRNA transcriptomes revealed the dysregulation of Wnt signaling (*frzb*/ola-miR-1–3p, *sfrp5*/ola-miR-96–5p/miR-455–5p) and bone morphogenetic protein (Bmp) signaling (*bmp3*/ola-miR-96–5p/miR-181b-5p/miR-199a-5p/miR-205–5p/miR-455–5p). Both pathways are major indicators of impaired bone formation, while the altered Rank signaling in osteoclasts (*c-fos*/miR-205–5p) suggests a potentially augmented bone resorption. Interestingly, a typical BaP-responsive pathway, the Nrf2-mediated oxidative stress response (*gst*/ola-miR-181b-5p/miR-199a-5p/miR-205), was also affected. Moreover, mRNA levels of epigenetic modification enzymes (e.g., *hdac6*, *hdac7*, *kdm5b*) were found dysregulated. The findings indicated that epigenetic factors (e.g., miRNAs, histone modifications) may di-

* Corresponding authors.
E-mails: bhrkong@cityu.edu.hk (R.Y.-C. Kong), frauke.seemann@tamucc.edu (F. Seemann).
** These authors contributed equally to this work.
*** The coauthor deceased on 7 February 2020.

https://doi.org/10.1016/j.jes.2022.04.051

rectly regulate the expression of genes associated with transgenerational BaP bone toxicity and warrants further studies. The identified candidate genes and miRNAs may serve as potential biomarkers for BaP-induced bone disease and as indicators of historic exposures in wild fish for conservation purposes.

Introduction

Polycyclic aromatic hydrocarbons (PAHs) are ubiquitously environmental pollutants that are predominantly formed by incomplete combustion of organic matters (Moffat et al., 2015). Moreover, accidental PAH pollution through oil spills has caused serious marine environmental impacts and toxic effects on marine organisms including fish (Paine et al., 1996; Xu et al., 2016).

As a model PAH, benzo[a]pyrene (BaP) has been frequently detected in different environmental compartments (e.g., air, soil, water, sediments), with concentrations up to 3.41 μg/L detected in surface water (see reviews in Mo et al., 2021). Waterborne parental BaP exposure caused craniofacial deformities and spinal curvature in the F1-F2 offspring of zebrafish and has been described as a transgenerational bone toxicant in medaka fish (Corrales et al., 2014; Seemann et al., 2015). BaP or its metabolites may impact F1 offspring via direct exposure of F1 germ cells in the gonads of F0 exposed fish. It is also possible that maternally transferred BaP from F0 exposed females is released during F1 embryogenesis and potentially impacts F2 offspring by interacting with the F2 primordial germ cells. Therefore, F3 represents the first transgenerational group of offspring without any exposure to BaP (Seemann et al., 2015; Skinner, 2008). Notably, increased vertebral compression of F1–F3 medaka larvae originating from the BaP-exposed F0 ancestors was associated with reduced osteoblast (OB) abundance and bone tissue at the vertebral centra (Seemann et al., 2015). Subsequent studies using unique transgenic medaka bone model confirmed that osteoblastic bone formation was impaired by ancestral BaP exposure (Mo et al., 2020). The regulatory regions of *collagen 10a1* and *osterix* (*osx*) were identified as candidates for inherited epigenetic modifications (Mo et al., 2020).

Transgenerational BaP bone impairment identified at the larval stages persisted into adulthood, as evidenced by a decreased vertebral bone thickness in F3 male fish, although F3 females were unaffected (Seemann et al., 2017). Bone-associated gene - miRNA pairs, such as *osx*/miR-214, *runt-related transcription factor 2* (*runx2*)/miR-204, were linked to this suppressed OB activity (Seemann et al., 2017). Moreover, in mice, paternal pre-conceptional BaP-exposure altered the miRNA and gene expression profiles of F1 embryos, revealing dysregulated miRNAs (e.g., mmu-miR-204, mmu-miR-181b, mmu-miR-210, etc.) associated with bone formation and dysregulated genes related to epigenetic mechanisms including DNA methyltransferases (*dnmt1, dnmt3a, dnmt3l*), histone deacetylases (*hdac1, hdac6, hdm1a*), *histone lysine demethylases* (*kdm4a, kdm4c*), and thymine DNA glycosilase (*tdg*) (Brevik et al., 2012a, 2012b). However, the full extent of dysregulated molecular pathways of bone metabolism, osteogenic miRNAs and epigenetic genes (i.e., genes encoding epigenetic regulators) following ancestral BaP exposure remains unclear.

Bone remodeling in mammals and fish is a continue process to maintain bone homeostasis and is characterized by the intimate interplay between OBs, the bone-forming cells and bone resorbing cells (osteoclasts; OCs) (Crockett et al., 2011). Development of OB and OC lineages, including commitment, proliferation, differentiation and maturation, are delicately controlled by the expression of transcription factors (*runx2, osx, atf4, nfatc1*), molecular signaling pathways (Wnt signaling, Bmp signaling, Rank signaling) and hormones (Crockett et al., 2011). Epigenetic factors such as miRNAs are closely involved in the regulation of bone metabolism (Kim and Lim, 2014).

MiRNAs are a set of small single-stranded RNAs that are typically 18–22 nucleotides in length and are vital for RNA silencing and post-transcriptional gene regulation. MiRNAs regulate gene silencing through complete or partial complementary binding to the 3′-untranslated regions (UTRs), 5′-UTRs and/or coding regions (CDS) of target mRNAs, thereby leading to translational repression or degradation of transcripts (mRNA cleavage) (Bartel, 2018). MiRNAs can regulate bone metabolism by targeting important regulators and marker genes of bone formation and resorption in vertebrates (Bellavia et al., 2019; Mo et al., 2021).

It is hypothesized that bone thinning in F3 male medaka – caused by F0 ancestral BaP exposure – is mediated by the dysregulation of bone miRNAs and their target genes. In the present study, the medaka bone model was used to: (1) determine alterations in OB abundance attributed to ancestral BaP exposure in the F3 adult male medaka vertebrae using histomorphometric analysis; (2) identify the molecular and epigenetic pathways, osteogenic genes, epigenetic genes, bone miRNAs, and gene – miRNA pairs dysregulated in F3 adult male vertebrae due to ancestral BaP exposure using RNA sequencing and small RNA sequencing. This study revealed impairment at the cellular level as well as dysregulated genetic and epigenetic pathways related to bone metabolism and oxidative stress in bone tissue of F3 adult male medaka with transgenerationally inherited BaP toxicity.

1. Materials and methods

1.1. *Multigenerational exposure experiments*

The double transgenic *col10a1*:nlGFP/*osx*:mCherry medaka line (Renn et al., 2013) was used in this study. All animal handling was performed following the regulations of the Animal Ethics Committee, City University of Hong Kong. As previously described in Mo et al. (2020), exposure of medaka fish

to various concentrations of BaP (0.001, 0.01, 0.1, 1 μg/L) were conducted in a preliminary exposure experiment, and that only BaP at 1 μg/L resulted in the transgenerational bone phenotype. A DMSO/ethanol solvent combination (DMSO and ethanol were mixed at a ratio of 1 to 4) was used to enhance the solubility of BaP for preparation of the BaP stock solution. In this study, fish (4-months old; 10 male/female pairs per replicate) were exposed to either 1 μg/L BaP (6 replication tanks) or 0.0005% DMSO-ethanol solvent (4 replication tanks) for 21 days. BaP concentrations in the tank water were randomly measured 24 hr after BaP administration (0.67 ± 0.15 μg/L). No BaP was detectable in F1 embryos of control and the treatment (Mo et al., 2020).

After multiple changes of water at experimental day 22 and day 23, a daily medaka embryo collection was performed from day 24 onwards for two weeks. Embryos were reared following the standard medaka rearing protocol to produce F1 and the subsequent F2 and F3 fish. In each tank, 15 pairs of fish were reared in water without the addition of BaP or carrier solvent. Medaka were cultivated at (26 ± 0.5)°C under a controlled cycle of 14 hr light: 10 hr dark and fed with dry flake food and brine shrimp nauplii.

1.2. Bone histomorphometry

Whole medaka fish were fixed after removal of fins, operculum, skull roof, and otoliths. Fixed samples were processed following our previously established protocol (Kong et al., 2008). Serial sections of individual fish were cut (7 μm) on a rotary microtome (Leica RM2125, Germany). Longitudinal sections showing vertebral columns were selected and number coded. OBs were identified by measuring alkaline phosphatase (ALPase) activity using the Goldner's Trichome modified staining as described previously (Shanthanagouda et al., 2014). Six sections containing vertebral segments 15–29 per fish ($n = 3$–4 per treatment) were selected to assess the OB abundance in the intervertebral segments (IVS) of F3 male fish under a microscopy (Nikon Eclipse 90i, Japan).

1.3. Transcriptomic analysis of F3 male medaka vertebrae

F3 male fish at an age of 6 months were anesthetized via hypothermic shock and their vertebrae were dissected. Muscle and notochord tissue were thoroughly removed from the bone tissue (Seemann et al., 2017). Vertebrae of five medaka from the same treatment tank were pooled as one replicate, and total RNA was extracted from each sample using the mirVana miRNA isolation kit (Applied Biosystems, USA). RNA concentration and quality were assessed using a NanoDrop 2000 (Thermo Fisher Scientific, USA) and a Bioanalyzer 2100 (Agilent Technologies, USA). Samples with an RNA integrity number (RIN) over 7 (7.4–8.2) were saved for RNA library construction ($n = 4$ per treatment). Paired-end reads (all 150 bp read length) were sequenced using an Illumina HiSeq platform at the Beijing Genomics Institute (BGI, China).

Raw reads were bioinformatically sorted and the resulting quality-trimmed reads (Phred score > 20) were retained and mapped to the Japanese medaka HdrR genome reference (ASM223467v1) using Hisat2. The read counts of genes were quantified using FeatureCounts and normalized using the fragments per kilobase million (FPKM) method (Liao et al., 2014). Transcripts with expression > 1 FPKM were subject to downstream differential expression analysis using the DESeq2 package in R (Zhang et al., 2016). Genes with an adj-p value < 0.05 (FDR < 0.05) were considered differentially expressed genes (DEGs) as described by Xu et al. (2016).

The identified medaka DEGs were converted to their human orthologs, followed by Gene Ontology (GO) functional enrichment analysis using the Database for Annotation, Visualization and Integrated Discovery (DAVID). Ingenuity Pathway Analysis (IPA, QIAGEN, USA) was employed to decipher the molecular pathways that were dysregulated by ancestral BaP exposure. For the GO analysis and IPA, a $p < 0.05$ was considered significant.

1.4. Analysis of small RNA transcriptome of F3 male medaka vertebrae

Total RNA was isolated from the pooled bone tissues (vertebrae of 5 fish in each replicate) for small RNA transcriptomic analysis. Eight libraries were generated for small RNA-seq; however, quality of two small RNA libraries were not satisfactory, so the remaining 6 small RNA libraries were used for the sequencing and downstream analysis. Libraries ($n = 3$ per treatment) were constructed as described in the previous study (Li et al., 2016). Single-end reads, each with a 50 bp read length, were sequenced on an Illumina HiSeq platform at BGI (BGI, China).

Raw reads were bioinformatically sorted and the resulting quality-trimmed reads (Phred score > 20) were retained for downstream analyses. The prediction of precursor miRNA and mature miRNA formation was conducted using miRDeep2 with the medaka genome (ASM223467v1) and all precursor miRNA and mature miRNA sequences from the miRBase database version 22.1 (www.mirbase.org) used as references. Predicted precursor miRNA and mature miRNA sequences were extracted using the parse platform. The sequence of each predicted miRNA was blasted against the miRBase database. Several criteria had to be met for a predicted miRNA to be considered as a known miRNA in the miRbase (Li et al., 2016): (1) used the same strand as the miRNA(s) in the miRbase; (2) shared at least 90% of its length with the miRNA(s) in the miRbase; (3) no indels were present in the predicted miRNA compared to the miRNA(s) in the miRbase; (4) the nucleotides 2–8 of the predicted miRNA were the same as those of the miRNA(s) in the miRbase; and (5) the number of mismatches was not more than 1 nucleotide between the predicted miRNA and its counterpart.

The quality-trimmed reads were mapped to the medaka genome using Bowtie (Langmead, 2010). The read counts of sequences were quantified against the predicted mature miRNAs using HTSeq-count (Anders et al., 2015). The relative abundance of these unique miRNAs was presented as the number of tabulated reads per million filtered reads (RPM) (Grün et al., 2014). Predicted miRNA sequences with expression ≥ 10 RPM in at least one sample were deemed as expressed miRNAs for the downstream analysis (Li et al., 2016). Differential expression of miRNAs was analyzed using the DESeq2 package in R. Identified miRNAs with the cutoff settings of a p value < 0.05 plus $\log_2$(fold change) < -1 or > 1 were con-

sidered differentially expressed miRNAs (DEMs) as described by Fu et al. (2020).

1.5. Integrated analysis of DEMs and DEGs

For miRNA target prediction, only canonical sites of miRNAs (e.g., offset 6mer, 6mer, 7mer-m8) that have 6–7 contiguous Watson–Crick pairs to the seed region of that miRNA (miRNA position nucleotides 2–8) were considered. Atypical canonical sites and noncanonical sites (imperfect seed match) were excluded (Bartel, 2009, 2018). The miRanda algorithm was applied to predict DEGs targeted by the identified DEMs (Li et al., 2016). Briefly, the sequences of 3′-UTRs, CDS and 5′-UTRs of DEGs were obtained from Ensembl (http://www.ensembl.org/index.html). The whole length of these miRNAs was aligned to the 3′-UTRs, CDS, and 5′-UTRs of genes based on the complementarity matches using dynamic programming alignment. Then the thermodynamic stability (the free energy, ΔG) of the mRNA – miRNA duplexes was calculated using the Vienna 1.3 RNAlib installed in the miRanda algorithm. Due to the fact that there is no universally accepted standard for default parameters and cutoffs defining miRNA-like hairpin structures among different prediction algorithms (Bartel, 2009, 2018; Peterson et al., 2014), the default parameters (i.e., Score $\geq$ 140 and Energy ≤ -7.0 kcal/mol) were used to select target candidate miRNA-gene pairs (Qiang et al., 2017). Additionally, two strict requirements were set for the selection of gene – miRNA pairs: (1) perfect alignments in the miRNA seed region at nucleotide position 2–8 (the key region for mRNA – miRNA recognition) to the proposed target mRNA sequences; (2) a negative expression relationship between DEM and DEG (i.e., up-DEMs/down-DEGs, down-DEMs/up-DEGs). The mRNA – miRNA regulation networks were depicted using IPA.

1.6. Expression validation of genes and miRNAs by qPCR

The expression of genes and miRNAs were validated using qPCR, and the methodological details are shown in the Appendix A Text S1.1 and S1.2.

1.7. Statistical analysis

The qPCR data were analyzed using GraphPad Prism 8 (GraphPad, USA) and are presented as mean ± SEM. Pearson correlation analysis was conducted on the F3 gene data generated by NGS and qPCR. A Student's *t*-test was used to compare the OB abundance and expression of genes and miRNAs in bone tissues of male fish in the control and the ancestral BaP treatment. A value of $p < 0.05$ was considered statistically significant (*).

2. Results

2.1. OB abundance

Histomorphometric analysis was performed to assess the medaka OB abundance of F3 male medaka potentially altered by ancestral BaP exposure. In longitudinal sections of the medaka vertebral column, cells in brown color (ALPase activity-positive after Goldner-Trichrome staining) around the osteoid were identified as OB (**Fig. 1a-d**). The number of OB in the intervertebral regions of segments 15–29 was significantly ($p < 0.05$) reduced (approximate 10.7% per IVS) in the F3 ancestrally BaP-treated fish in comparison with the F3 control (**Fig. 1e**).

2.2. Transcriptome sequencing analysis

The transcriptome analysis yielded an average of 73.9 million clear reads in F3 medaka bone samples, and the average mapping rate was 88.3% (Appendix A **Table S1**). A total of 1094 DEGs were identified at FDR < 0.05, which includes 731 upregulated DEGs and 363 downregulated DEGs (data not shown).

2.3. GO enrichment analysis and ingenuity pathway analysis (IPA)

GO enrichment analysis on the identified DEGs were performed and presented in Appendix A **Fig. S1a–c**. IPA of the transcriptome highlighted canonical pathways related to I) bone metabolism such as signaling by Rho family GTPases, integrin signaling, RhoA signaling, Rank signaling in OCs, protein ubiquitination pathway, Bmp signaling pathway, and the role of OBs, OCs, and chondrocytes in rheumatoid arthritis and II) typical BaP-responsive signaling pathways, such as Nrf2-mediated oxidative stress response, aryl hydrocarbon receptor (AhR) signaling, and xenobiotic metabolism signaling (**Table 1** and Appendix A **Table S2**). Notably, although many key genes of these BaP-responsive signaling pathways (e.g., *ahr, nrf2, cyps*) were not differentially expressed, several other DEGs in these pathways were significantly enriched (**Table 1**), strongly indicating the activation (a positive Z-score in IPA) of these pathways upon ancestral BaP exposure.

The majority of genes enriched in bone metabolism pathways were associated with Wnt signaling and Bmp signaling (as a part of the role of OBs, OCs, and chondrocytes in rheumatoid arthritis; **Table 1**). Genes including *bmp3, dkk3b, sfrp5, frzb, gsk3ba*, and *csnk1a1* were upregulated. Ubiquitin poses an essential regulatory role in the Wnt pathway, and genes of the protein ubiquitination pathway including *psma6b, rbx1, ube2ka*, and *usp2a* were upregulated (**Table 1**). All these genes may play active roles in the inhibited bone formation.

The Rank signaling in OCs, where 9 genes including *chp1, gsna, ppp3r1*, and *c-fos* were upregulated (**Table 1**), was potentially associated with the genetic dysregulation of bone metabolism in response to ancestral BaP exposure. Upregulated genes encoding actin (*actc1a, actb, actg1, actr2a, actr3b*), actin-related protein 2/3 protein complex (*arpc2, arpc3*), the Rho family small GTPase Cdc42 effector protein (*cdc42ep3, cdc42ep5*), Rho family of GTPases (*rhoua, rnd2*), and integrin $\beta-1$ (*itgb1b.1*) were enriched in the signaling of Rho family GTPases, integrin signaling, and RhoA signaling pathways. The upregulation of genes encoding V-ATPase (*atp6v0c, atp6v0e2, atp6v1f*), Rab family GTPase (*rab5ab, rab5c, rab7a*), cathepsin-L (*ctsl*), CAII (*cahz*), and MMP2 (*mmp2*) suggest a supporting role in bone resorption (Appendix A **Table S2**).

Expression of genes enriched in BaP-responsive pathways was significantly changed in the transgenerationally inherited BaP-induced bone toxicity. Genes including *gsto2, gstr, mgst1.2,*

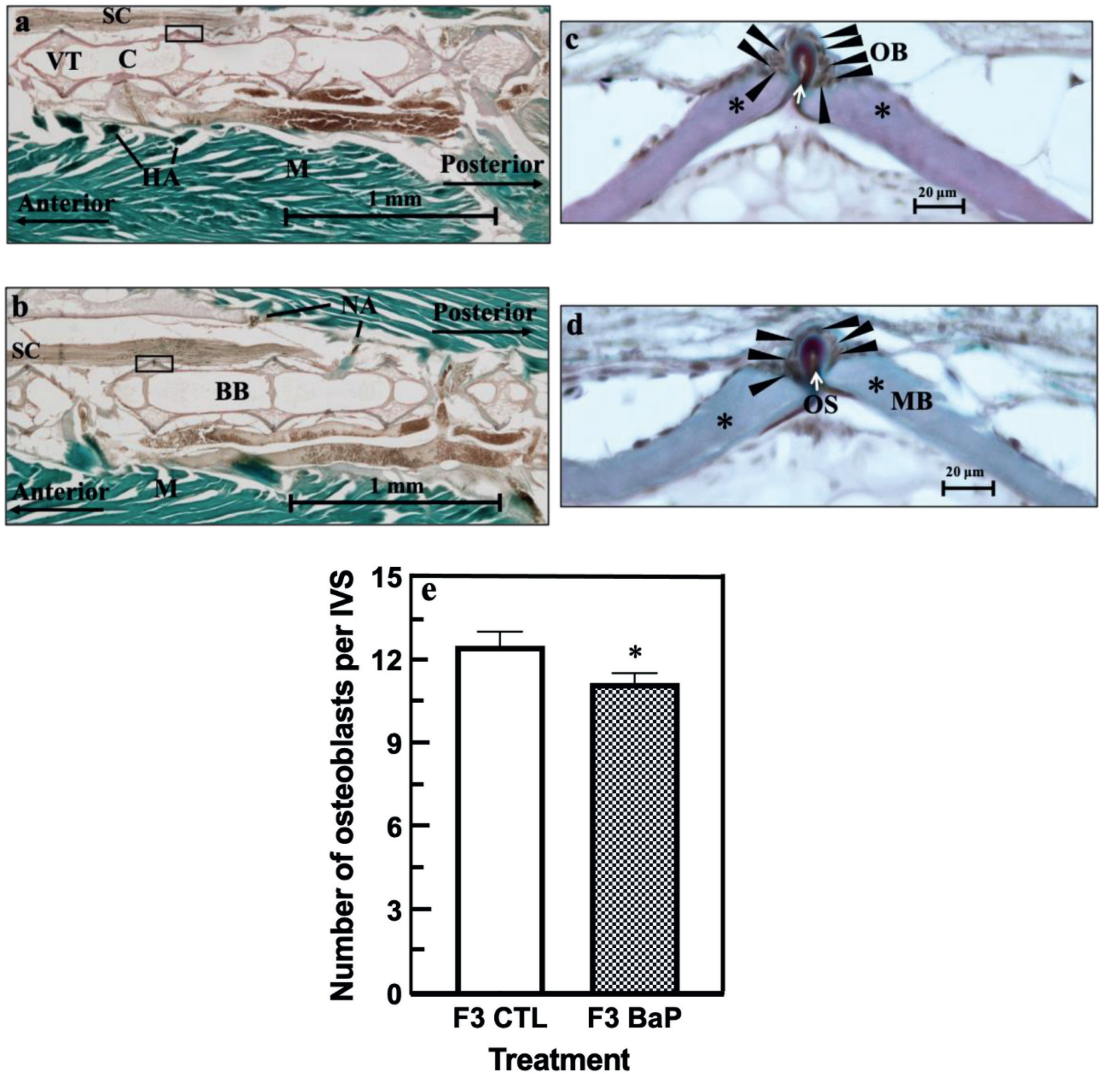

Fig. 1 – Ancestral benzo[a]pyrene (BaP) exposure reduced osteoblast abundance in vertebrae of F3 adult male fish assessed using Goldner's Trichrome staining. In the representative pictures, black arrows in the anterior and posterior indicate the head and tail region of the fish, respectively. Labels including M (muscle), SC (spinal cord), BB (back bone), NA (neural arch), HA (hemal arch), VT (vacuolated tissue), C (centrum), OB (osteoblasts; cells in brown color that are indicated using black arrowheads), OS (osteoid indicated by white arrows) and MB (mineralized bone indicated by asterisks) in the F3 control (a, c) and F3 ancestral BaP-exposed fish (b, d) were marked. (e) A bar chart showing the abundance of osteoblasts in the intervertebral segments (IVS) 15–29. Data are presented as mean ± SD ($n = 3–4$). *$p < 0.05$, according to Student's *t*-test. (For interpretation of the references to colour in this figure legend, the reader is referred to the web version of this article.)

c-fos were upregulated in the Nrf2-mediated oxidative stress response (**Table 1**). In addition, *aldehyde dehydrogenases* (e.g., *aldh4a1 aldh6a1, aldh7a1*) were upregulated in the AhR signaling (**Table 1**).

Moreover, the transcriptomic analysis revealed epigenetic regulator genes to be involved in the dysregulation of bone metabolism in F3 BaP male fish. Out of these, 8 genes including *hdac6, hdac7, kdm5b, jarid2, smyd3*, and *kat6b* were downregulated, while 2 genes (*prmt1, prmt6*) were upregulated.

The effects (activation or inhibition) of common upstream regulators for genes, which revealed significant expression changes in bone tissue upon ancestral BaP-exposure, were predicted using IPA. Namely, the transcription regulator genes *c-fos* and *kdm5b*, the enzyme encoded by *prmt1*, and non-coding RNA miR-205–5p were predicted to regulate bone metabolism genes (*itgb1b.1, cahz, mmp2, frzb, gsk3ba*), oxidative stress response genes (*mgst1.2*), and epigenetic genes (*hdac6*) (Appendix A **Fig. S2**).

2.4. *Small RNA sequencing analysis*

The small RNA sequencing analysis yielded an average of 18 million clear reads and the average mapping rate was 34.4% (Appendix A **Table S3**). A total of 918 miRNAs were identified (data not shown), which includes 341 sequences annotated to known sequences from other organisms and 577 sequences (novel miRNA candidates) not reported in miRBase22. In total, 7 DEMs were identified (ola-miR-205–5p, ola-miR-96–

Table 1 – Canonical pathways of Ingenuity Pathway Analysis (IPA) ($p < 0.05$) altered by ancestral benzo[a]pyrene exposure in F3 adult male bone tissue.

IPA Pathways	*p* Value	Z-score	Up-regulated genes	Down-regulated genes
Nrf2-mediated oxidative stress response	9.5×10^{-8}	2.67	*actc1a, actb, actg1, cct7, dnaja4, c-fos, fth1b, gsk3ba, gsto2, gstr, hars, hspb8, jund, mapk1, mapk9, mgst1.2, prdx1, rap2ab, rbx1, stip1, ube2ka, vcp*	*maf, prkcg*
Signaling by Rho family GTPases	3.0×10^{-6}	3.84	*actc1a, actb, actg1, actr2a, actr3b, arpc2, arpc3, cdc42ep3, cdc42ep5, cfl2, desma, ezr, c-fos, gna13b, gng5, itgb1b.1, mapk1, mapk12a, mapk9, myl9a, rhoua, rnd2, septin14*	*citb, gfap*
Integrin signaling	3.1×10^{-6}	3.27	*actc1a, actb, actg1, actr2a, actr3b, arf5, arpc2, arpc3, capn2, capns1b, cav1, cttn, gsk3ba, gsna, hras, itgb1b.1, mapk1, myl9a, parvb, rap2ab, rhoua, rnd2, tspan2b*	–
RhoA signaling	9.3×10^{-6}	3.50	*actc1a, actb, actg1, actr2a, actr3b, arpc2, arpc3, cdc42ep3, cdc42ep5, cfl2, ezr, gna13b, lpar3, myl9a, septin14*	*cit*
Role of osteoblasts, osteoclasts and chondrocytes in rheumatoid arthritis	0.001	NA	*bmp3, chp1, csnk1a1, dkk3b, c-fos, frzb, gsk3ba, gsna, itgb1b.1, mapk1, mapk12a, mapk9, ngfra, ppp3r1, sfrp5*	*csf1r, il1rapl2, nfat5b*
Protein ubiquitination pathway	6.0×10^{-5}	NA	*dnajc25, eloca, hspb8, hspb11, psma6b, psmb1, psmb2, psmb3, psmb4, psmb8, psmb9, psmc2, psmc3, psmd11b, psmd14, psmd3, psme1, rbx1, ube2ka, ube2l3, usp2a*	*nedd4l, ube2t, usp3*
Aryl hydrocarbon receptor signaling	0.015	1.00	*aldh4a1, aldh6a1, aldh7a1, c-fos,* gsto2, *gstr, mapk1, mgst1.2, ptges3b*	*aldh3a1, smarca4*
Xenobiotic metabolism signaling	0.032	NA	*aldh4a1, aldh6a1, aldh7a1, gsto2, gstr, hras, mapk1, mapk12a, mapk9, mgst1.2, ppp2cb, ptges3b, rap2ab, rbx1*	*aldh3a1, maf, prkcg*
Bmp signaling pathway	0.034	2.65	*bmp3, hras, mapk1, mapk12a, mapk9, prkar1ab, rap2ab*	–
Rank signaling in osteoclasts	0.040	2.65	*chp1, c-fos, gsna, mapk1, mapk12a, mapk9, ppp3r1*	–

Positive Z-score, negative Z-scores, and NA (not applicable) suggests an activated pathway, a suppressed pathway, and a pathway with unknown activity, respectively. A dash (–) indicates no up- or down-regulated genes in a specific IPA pathway.

5p, ola-miR-1–3p, ola-miR-455–5p, ola-let-7b, ola-miR-199a-5p, ola-miR-181b-5p), and all were downregulated (Appendix A **Table S4**).

2.5. In silico *analysis of miRNA-genes targets*

A total of 620 pairs of mRNA/miRNA clusters were predicted (data not shown). Pairs of mRNA/miRNA potentially related to bone metabolism and oxidative stress were shown in Appendix A **Table S5**.

2.6. *Construction of mRNA – miRNA molecular pathways*

Based on the *in-silico* analysis, the DEMs were incorporated into the molecular networks through IPA pathway construction. For the decreased bone formation, *bmp3* was predicted to be regulated by ola-miR-455–5p, ola-miR-181b-5p, ola-miR-96–5p, ola-miR-199a-5p, and ola-miR-205 in the Bmp pathway (Appendix A **Fig. S3a**), while *sfrp5* and *frzb* was predicted to be targeted by ola-miR-96–5p/miR-455–5p and ola-miR-1–3p, respectively, in the Wnt pathway (Appendix A **Fig. S3a**). By contrast, under osteoclastic bone resorption, *c-fos* was predicted to be targeted by ola-miR-205–5p in Rank signaling in OCs (Appendix A **Fig. S3b**) and Nrf2-mediated oxidative stress pathway (Appendix A **Fig. S3c**). Additionally, *gstr* was predicted to be regulated by ola-miR-181b-5p, ola-miR-199a-5p and ola-miR-205–5p in the Nrf2-mediated oxidative stress pathway (Appendix A **Fig. S3c**).

2.7. *Validation of gene and miRNA expression*

Selected key genes and miRNAs were evaluated in F1, F2 and F3 male medaka vertebrae using qPCR (**Fig. 2**). The F3 qPCR gene data were in agreement with the RNA-seq data described above (Pearson correlation efficiency: $r = 0.838$–0.931, $p < 0.001$; Appendix A **Fig. S4**). In bone tissues of F1, F2 and F3 male fish, *frzb, c-fos* and *gstr* were consistently upregulated (**Fig. 2a, c, e**), while ola-miR-1–3p was consistently downregulated (**Fig. 2b, d, f**).

3. Discussion

Exposure of F0 ancestors to BaP was demostrated to result in impaired bone formation in F3 medaka embryos and larvae (Mo et al., 2020; Seemann et al., 2015). Impairment of bone tissue persist to adulthood in male fish, but the underlying causes at the transcriptional level remained to be elucidated (Mo et al., 2020; Seemann et al., 2017). In the present study, novel data revealing reduced OB abundance and dysregulated molecular signaling pathways are presented. Two major pathway clusters were associated with the transgenerational inheritance of bone thinning in F3 adult male medaka induced by ancestral BaP exposure at an environmentally realistic level: (1) bone metabolism pathways and (2) BaP-responsive signaling pathways. Warranting further functional analysis, these two pathway clusters are potentially subject to the regulation of miRNAs and histone tail modification enzymes.

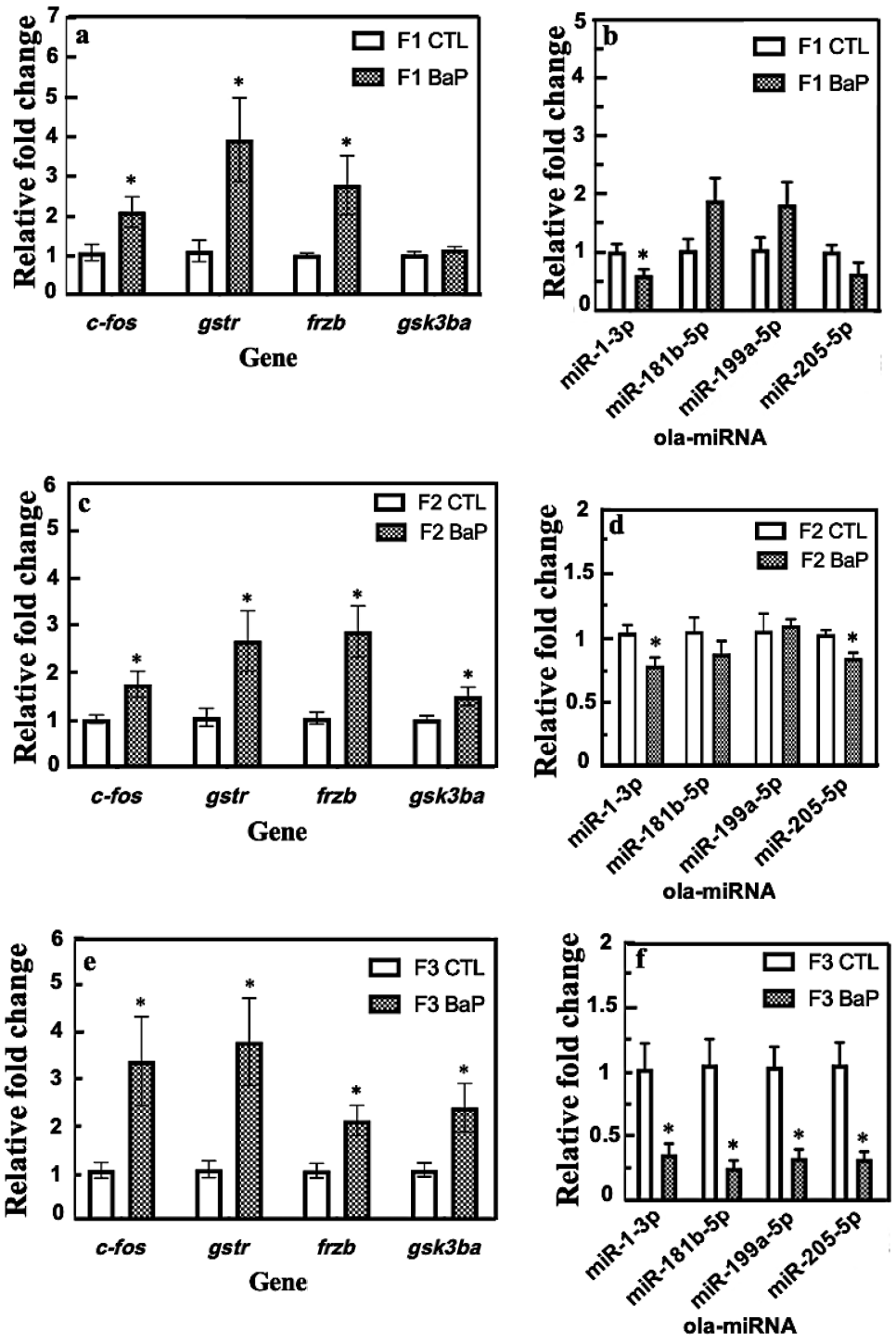

Fig. 2 – Dysregulation of bone genes and miRNAs by ancestral benzo[a]pyrene exposure in F1-F3 adult male medaka bone tissues. The expression of genes (a, c, e) and miRNAs (b, d, f) were validated using quantitative polymerase reaction chain (qPCR). Data are presented as means ± SEM ($n = 4$ pools per treatment). *$p < 0.05$, according to Student's *t*-test.

3.1. *Dysregulation of bone metabolism in the F3 generation*

The former cluster includes the activation of the Wnt signaling pathway, Bmp signaling pathway, Rank signaling in OCs, RhoA signaling, integrin signaling, and the signaling by Rho family GTPases, which most likely resulted in impaired bone formation and/or potentially augmented bone resorption in the F3 male fish upon ancestral BaP exposure. Due to the tight interplay of OBs and OCs, these results raise the question whether OB or OC pathways were initially affected, and which one may be considered a downstream effect. Previous findings and our data presented here suggest that ancestral BaP exposure impairs OB differentiation and maturation, causing

the dysfunction of OB-OC communication and the disruption of bone remodeling, and subsequently reduced bone quality and incremental microfractures (Mashiba et al., 2001; Mo et al., 2020).

The GO analysis and IPA identified key genes involved in the ancestrally BaP-exposure-induced bone toxicity. Notably, these genes regulate two pathways crucial for OB differentiation: the Wnt signaling pathway (non-canonical and canonical) and Bmp signaling pathway. FRZB, SFRP and DKK are extracellular antagonists of Wnt activation. The upregulation of *frzb* and *sfrp5* expression may reduce the binding of Wnts to low density lipoprotein-related protein (LRP) and frizzled receptors (Kobayashi et al., 2016). DKK3, unlike typical DKK such as DKK1 and DKK2, is unable to inhibit Wnt signaling (del Barco Barrantes et al., 2006), suggesting that upregulated *dkk3* may play a minor role in the altered Wnt signaling pathway. Deficiency in Wnt pathway activation possibly results in cytoplasmic β-catenin complex destruction (Appendix A **Fig. S3a**), as suggested through the upregulation and activation of *gsk3b* and *ck1* (*csnk1a1*), and consequently inhibiting the β-catenin-dependent transcription of bone formation genes (Wang et al., 2014). Wnt/β-catenin signaling is heavily involved in the commitment of mesenchymal stem cells (MSCs) to osteochondral progenitor cells, the proliferation and differentiation of premature OBs, and the survival/apoptosis of mature OBs, thereby indirectly regulating the differentiation and activation of OCs by controlling OPG and RANKL expression (Baron and Rawadi, 2007; Qiang et al., 2010). Overexpression of β-catenin in differentiated mouse OBs resulted in excess bone formation, while OB-specific deletion of β-catenin caused low bone mass by increased OC activity (Glass et al., 2005). These published data support the assumption that the transgenerational BaP-induced bone toxicity is mediated through altered Wnt signaling.

In addition, BMPs have been shown to promote osteogenesis via either Smad-dependent or Smad-independent signaling pathways (Bragdon et al., 2011). As the most abundant bone BMP produced by OBs, BMP3 (osteogenin) can negatively regulate bone density by antagonizing the activity of canonical BMPs (e.g., BMP2, BMP7) in the promotion of OB differentiation (Bragdon et al., 2011; Daluiski et al., 2011). Overexpression of BMP3 suppressed OB differentiation both *in vitro* and *in vivo* (Kokabu et al., 2012; Daluiski et al., 2001). Impairment of OB differentiation (Mo et al., 2020) and bone metabolism caused by transgenerational BaP exposure is likely associated with the upregulation of *bmp3* in the Bmp signaling pathway (Appendix A **Fig. S3a**).

A potential increase in osteoclastogenesis was suggested by the positive Z-scores for Rank signaling in osteoclasts (Appendix A **Fig. S3b)**, RhoA signaling, integrin signaling, and signaling by Rho family GTPases (**Table 1**). Enhanced osteoclastogenesis may contribute to the inherited bone thinning, especially when bone formation is inhibited by ancestral BaP exposure, which suggests that bone repair and remineralization are possibly compromised (Renn et al., 2013). Although only low OC numbers were reported on the vertebral centra during normal bone development and metabolism in medaka (most OCs were present on the arches) (Chatani et al., 2011), ectopic osteoclastic resorption could be induced experimentally on medaka vertebrae (Yu et al., 2016). Typical bone resorption genes, such as *tracp, ctsk*, and *mmp9*, were not dysregulated at the transcriptional level except for *c-fos, cahz*, and *mmp2*. Therefore, the potential increase in osteoclastogenesis may be orchestrated through BaP-activated AhR signaling on Rank/c-Fos/NFATc1 signaling (Iqbal et al., 2013; Izawa et al., 2016). Whether augmented OC abundance and/or OC activity on the vertebral centra in F3 adult male medaka is directly induced by ancestral BaP exposure remains to be determined. The developmental origins of the phenotype presented in this study suggest the defective OB differentiation, and thus, a lack of mature OBs and, as a consequence, reduced OB activity are primarily responsible for the adult bone thinning.

3.2. *Regulation of bone metabolism through xenobiotic-responsive pathways*

Activation of the typical BaP-responsive canonical pathways (Van Kesteren et al., 2013), including AhR signaling, and Nrf2-mediated oxidative stress response (**Table 1**), was present in F3 male bone tissues upon ancestral BaP exposure.

As phase II biotransformation enzymes, GSTs catalyze the conjugation of reduced glutathione to reactive electrophiles of metabolized chemicals, while ALDHs remove toxic aldehydes generated from oxidative stress and lipid peroxidation induced by BaP exposure (Moffat et al., 2015). Genes encoding glutathione S-transferase (*gstr, mgst1.2*) and ALDH (*aldh4a1, aldh7a1*) were upregulated, which supports the assumption of the persistence of a BaP toxicity response in the F3 generation. However, the BaP metabolism marker genes (e.g., *ahr, nrf2, cyp1a1, cyp1b1*) were not differentially expressed in transgenerational BaP-exposed male fish. Since no direct BaP exposure or metabolism of BaP occurred in the F3 generation (Mo et al., 2020), it is unclear why the Nrf2-mediated oxidative stress response signaling was activated (Appendix A **Fig. S3c**). One possibility is that the expression of these DEGs (e.g., *gstr, mgst1.2, aldh4a1, aldh7a1*) was under the direct regulation of epigenetic factors that are transmitted through several generations (discussed in section 3.4). Nonetheless, the Nrf2-mediated oxidative stress response remains to be verified at the cellular or tissue level (e.g., measurement of antioxidant content and antioxidant enzyme activity). However, we cannot rule out the possibility that these genes (e.g., *gstr, mgst1.2, aldh4a1, aldh7a1*) may also be involved in other biological processes.

Taken together, the histomorphometric and transcriptomic data presented in this study provide a mechanistic understanding of bone defects induced by ancestral BaP exposure. Based on the existing literature and the findings presented in this study, a molecular regulatory network underlying the transgenerational BaP bone toxicity is proposed here (**Fig. 3**). The activation of AhR signaling may suppress MSC commitment to the OB lineages through inhibiting the Wnt/β-catenin pathway (Tong et al., 2017). Moreover, AhR activation can modify β-catenin levels by promoting β-catenin ubiquitination and degradation (Ohtake et al., 2007). Thus, AhR activation possibly inhibits bone formation by reducing β-catenin proteins without changing its transcriptional activity (Schneider et al., 2014; Yu et al., 2018). Inhibitory effects of AhR signaling on bone formation may also be induced through suppression of the Bmp signaling pathway. Indeed, it has been shown that BaP exposure suppressed the BMP2-induced MSC

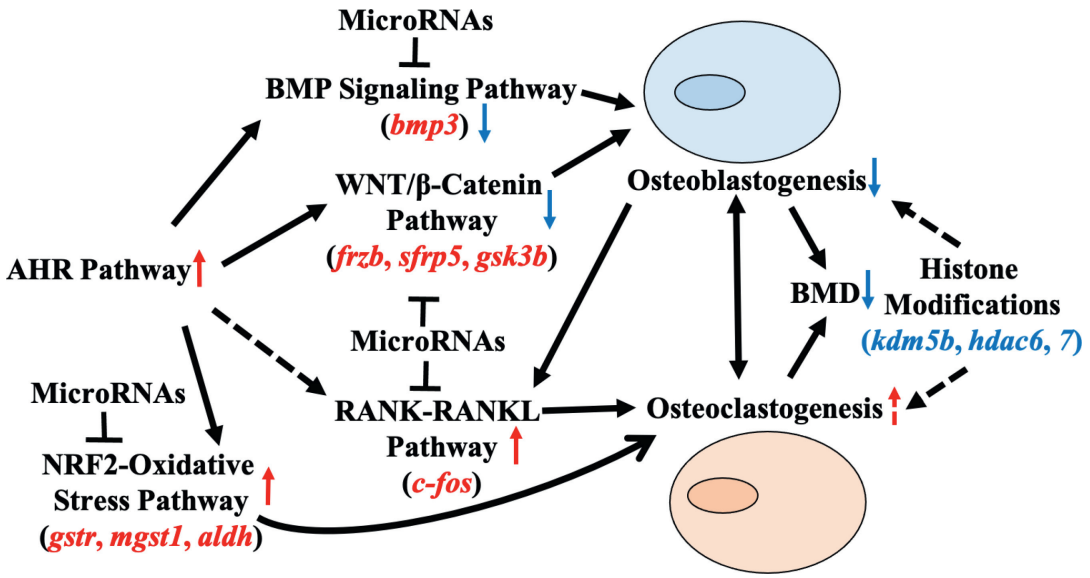

Fig. 3 – Hypothetical molecular regulatory networks of osteoblastogenesis and osteoclastogenesis in the transgenerational benzo[a]pyrene bone toxicity in F3 adult male medaka. AHR: aryl hydrocarbon receptor; BMD: bone mineral density; BMP: bone morphogenetic protein; NRF2: nuclear factor-erythroid factor 2-related factor 2; RANK: Receptor activator of nuclear factor κB; RANKL: receptor activator of nuclear factor κB ligand.

differentiation and the BMP2/Smad1/5/8 signaling pathway through activation of the AhR, downregulation of BMPRII and upregulation of Hey1 (An et al., 2020). Moreover, the activation of AhR signaling and the subsequently increased crosstalk between the AhR signaling pathway and the Rank-Rankl signaling pathway promotes OC differentiation (Omata et al., 2015; Izawa et al., 2016). This can interfere with the balance of OBs and OCs and aggravate bone resorption (Iqbal et al., 2013; Yu et al., 2015).

Activation of the AhR signaling pathway may indirectly modify bone metabolism through the induction of oxidative stress/Nrf2 signaling. The Nrf2 signaling pathway is emerging as a key factor in regulating bone metabolism despite its seemingly ambiguous role. Levels above the physiological steady state affected bone remodeling, resulting in reduced bone thickness and strength (Hinoi et al., 2006; Sun et al., 2015). Oxidative stress breaks the redox balance through changing the glutathione/ glutathione disulfide ratio, which may affect the expression of bone-relevant transcription factors (Jones et al., 2002). Downstream genes such as *gst* and *aldh* have been shown to be involved in inhibition of OB proliferation and decrease bone formation (Hoshi et al., 2012; Mlakar et al., 2012).

3.3. *Epigenetic regulation of BaP-induced transgenerational bone impairment*

Genes coordinating bone metabolism (e.g., *wnt, bmp, runx2, osx, rank, opg, nfatc1*) have been shown to be transcriptionally or post-transcriptionally regulated by miRNAs or have their chromatin structure modified by epigenetic enzymes such as DNA methyltransferases, histone methyltransferases, histone demethylase, and histone deacetylases (Bellavia et al., 2019).

The identified DEMs (e.g., ola-miR-1–3P, ola-miR-96, ola-miR-181b-5p, ola-miR-199a-5p) have possible regulatory roles in the inhibited bone formation and augmented bone resorption in transgenerationally inherited BaP-induced bone toxicity. For instance, downregulation of miR-1–3p may inhibit OB differentiation via upregulation of gene encoding HIF-1 alpha inhibitor (Zhou et al., 2020). Moreover, miRNA-96 promoted OB differentiation and bone formation via targeting *sost* and activating the Wnt signaling pathway (Ma et al., 2019). Overexpression of miRNA-181a/b-1 enhanced osteogenesis by targeting Pten/PI3K/Akt signaling (Zheng et al., 2019). Furthermore, the overexpression of miR-199a-5p promotes OB maturation via suppressing HIF1A-TWIST1 pathway, while a reduction in miR-199a-5p by siRNA treatment inhibits OB differentiation (Chen et al., 2015).

HDACs are transcriptional co-repressors of gene expression (Ghayor et al., 2016). The shift of MSCs toward adipocytes is controlled by HDACs (McGe-Lawrence et al., 2016). Expression of HDAC6 and HDAC7 (encoded by *hdac6* and *hdac7*, respectively) negatively regulated osteoblastogenesis (Westendorf et al., 2002; Jensen et al., 2008) and osteoclastogenesis (Destaing et al., 2005; Jin et al., 2013). Histone H3 lysine4 demethylase encoded by *kdm5b* could inhibit the transcription of genes regulating the self-renewal of MSCs and bone cell differentiation (Han et al., 2017). Notably, expression of KDM5B can inhibit the osteoblastic lineage commitment and activity of hematopoietic stem cells (Cellot et al., 2013; Bustos et al., 2018).

Intriguingly, the expression of *frzb, c-fos* and *gstr* (upregulated) and ola-miR-1–3p (downregulated), was found conserved in the F1, F2 and F3 generation with ancestral BaP exposure (**Fig. 2a–f**). Thus, they are candidates as potential triggers of the bone impairment in the offspring due to ancestral BaP exposure. Moreover, they should be considered as priority

targets for possible epigenetic modifications, warranting further study. Follow-up functional studies (e.g., *in vitro* miRNA – mRNA interaction luciferase reporter assay, gene knock-out/knock-in) are required to elucidate the specificity of interactions between the candidate genes (e.g., *frzb*) and miRNAs (e.g., ola-miR-1–3p) as well. These future studies will detail how modification of the identified miRNAs will impact the Wnt and Bmp pathways and their association with the transgenerational BaP bone phenotype in male fish.

3.4. *Transgenerational inheritance of BaP-induced bone toxicity in male offspring*

The observed transgenerational bone phenotype in male offspring was possibly transmitted through epigenetic modifications (e.g., ncRNA, DNA methylation, histone modifications) of the parental gametes in response to ancestral BaP exposure (Godschalk et al., 2018; McPherson et al., 2014; Vanhees et al., 2014). The mechanism by which epigenetic information is transmitted from one generation to the next generation may be related to the RNA content of gametes. For example, it has been showed that microinjection of RNA (e.g., RNA fragments, miRNAs) into sperm affected the inheritance of tail color, induced heart malformation and altered body size in the offspring of mice (Grandjean et al., 2009; Rassoulzadegan et al., 2006; Wagner et al., 2008). BaP exposure has been reported to alter the RNA content of sperm and the DNA methylation pattern in mouse testes (Godschalk et al., 2015). Additionally, expression of mRNA and miRNA was significantly modified in mouse embryos with paternal BaP exposure (Brevik et al., 2012a, 2012b). The altered RNA content of sperm could possibly modify postfertilization events and embryonic development, exerting long lasting effects on the individuals (Rando, 2016).

In the present study, the dysregulation of miRNAs (e.g., miR-1–3p) in F1-F3 male medaka ancestrally exposed to BaP could potentially exert such reprogramming effects and potentially lead to the transgenerational bone phenotype. Indeed, epigenetic information including ncRNA and chromatin proteins have been shown to be transgenerationally transmitted (Rando, 2016; Rassoulzadegan et al., 2006). It is inferred that the dysregulated miRNAs (e.g., miR-1–3p) in the present study may serve as a sperm-related factor inducing the transgenerational bone toxicity phenotype, or these miRNAs and/or genes (e.g., *gstr, frzb, c-fos*) were differentially regulated by other transmittable epigenetic factors (e.g., DNA methylation and/or histone modifications) during early development of the fish embryos after ancestral exposure to BaP. Therefore, the potential roles of DNA methylation and histone modifications in transgenerational BaP bone toxicity remain to be elucidated. Moreover, it is unclear whether the dysregulation of genes and miRNA in F1-F3 generations is male-specific or whether it also occurs in female fish without affecting the bone at the tissue level, warrants further investigations.

4. Conclusions

The observed reduction in OB abundance, enrichment of bone metabolism and BaP-responsive pathways, and mRNA – miRNA molecular regulatory networks suggest that reduced bone formation and potentially increased bone resorption are being causative for the previously reported ancestral BaP-exposure induced transgenerational bone phenotype. The enriched signaling pathways, predicted upstream regulators, and constructed miRNA – mRNA molecular regulatory networks suggest a major role of reduced bone formation and minor actions of increased bone resorption underlying the transgenerational BaP bone toxicity. The inherited dysregulation of genes and enriched signaling pathways of osteoblastogenesis and osteoclastogenesis were possibly orchestrated through changed miRNA expression and epigenetic enzyme modifications. Further studies are required for clarifying the potential modifications of ancestral BaP exposure on the epigenetic profiles (DNA methylation and histone modifications) of F3 adult axial skeleton. Medaka models are promising tools for deciphering the epigenetic mechanisms of transgenerational BaP bone toxicity. The dysregulated genes/miRNAs identified may serve as potential biomarkers for ancestral BaP exposure and possible bone impairment in wild fish populations for environmental health assessment, warranting functional studies.

Data Availability Statement

The RNA sequencing raw data of this study have been submitted to the NCBI Sequence Read Archive (SRA) (http://www.ncbi.nlm.nih.gov/sra) under the accession number PRJNA757563.

Declaration of Competing Interest

The authors declare that they have no known competing financial interests or personal relationships that could have appeared to influence the work reported in this paper.

Acknowledgments

This work was supported by the Southern Marine Science and Engineering Guangdong Laboratory (Guangzhou) (No. SMSEGL20SC02), the National Natural Science Foundation of China (No. 41977371), and a Project grant from the Shenzhen and Technology Innovation Commission (No. JCYJ20170818094137791). Dr. Seemann was supported by the National Institute of Environmental Health Sciences of the National Institutes of Health under award number 1R15ES032936–01.

Appendix A Supplementary data

Supplementary data associated with this article can be found in the online version at doi:10.1016/j.jes.2022.04.051.

REFERENCES

An, L., Shi, Q., Fan, M., Huang, G., Zhu, M., Zhang, M., et al., 2020. Benzo[a]pyrene injures BMP2-induced osteogenic

differentiation of mesenchymal stem cells through AhR reducing BMPRII. Ecotoxicol. Environ. Saf. 203, 110930.
Anders, S., Pyl, P.T., Huber, W., 2015. HTSeq—A python framework to work with high-throughput sequencing data. Bioinformatics 31 (2), 166–169.
Baron, R., Rawadi, G., 2007. Targeting the Wnt/β-catenin pathway to regulate bone formation in the adult skeleton. Endocrinology 148 (6), 2635–2643.
Bartel, D.P., 2009. MicroRNAs: target recognition and regulatory functions. Cell 136 (2), 215–233.
Bartel, D.P., 2018. Metazoan microRNAs. Cell 173 (1), 20–51.
Bellavia, D., De Luca, A., Carina, V., Costa, V., Raimondi, L., Salamanna, F., et al., 2019. Deregulated miRNAs in bone health: epigenetic roles in osteoporosis. Bone 122, 52–75.
Bragdon, B., Moseychuk, O., Saldanha, S., King, D., Julian, J., Nohe, A., 2011. Bone morphogenetic proteins: a critical review. Cell Signal. 23 (4), 609–620.
Brevik, A., Lindeman, B., Brunborg, G., Duale, N., 2012a. Paternal benzo[a]pyrene exposure modulates microRNA expression patterns in the developing mouse embryo. Int. J. Cell Biol. 2012, 407431.
Brevik, A., Lindeman, B., Rusnakova, V., Olsen, A.K., Brunborg, G., Duale, N., 2012b. Paternal benzo[a]pyrene exposure affects gene expression in the early developing mouse embryo. Toxicol. Sci. 129 (1), 157–165.
Bustos, F., Sepúlveda, H., Prieto, C.P., Carrasco, M., Díaz, L., Palma, J., et al., 2018. Runt-related transcription factor 2 induction during differentiation of wharton's jelly mesenchymal stem cells to osteoblasts is regulated by jumonji at-rich interactive domain 1B histone demethylase. Stem Cells 35 (12), 2430–2441.
Cellot, S., Hope, K.J., Chagraoui, J., Sauvageau, M., Deneault, E., MacRae, T., et al., 2013. RNAi screen identifies Jarid1b as a major regulator of mouse HSC activity. Blood 122 (9), 1545–1555.
Chatani, M., Takano, Y., Kudo, A., 2011. Osteoclasts in bone modeling, as revealed by in vivo imaging, are essential for organogenesis in fish. Dev. Biol. 360 (1), 96–109.
Chen, X., Gu, S., Chen, B.F., Shen, W.L., Yin, Z., Xu, G.W., et al., 2015. Nanoparticle delivery of stable miR-199a-5p agomir improves the osteogenesis of human mesenchymal stem cells via the HIF1a pathway. Biomaterials 53, 239–250.
Corrales, J., Thornton, C., White, M., Willett, K.L., 2014. Multigenerational effects of benzo[a]pyrene exposure on survival and developmental deformities in zebrafish larvae. Aquat. Toxicol. 148, 16–26.
Crockett, J.C., Rogers, M.J., Coxon, F.P., Hocking, L.J., Helfrich, M.H., 2011. Bone remodeling at a glance. J. Cell Sci. 124 (7), 991–998.
Daluiski, A., Engstrand, T., Bahamonde, M.E., Gamer, L.W., Agius, E., Stevenson, S.L., et al., 2001. Bone morphogenetic protein-3 is a negative regulator of bone density. Nat. Genet. 27 (1), 84–88.
del Barco Barrantes, I., Montero-Pedrazuela, A., Guadano-Ferraz, A., Obregon, M.J., De Mena, R.M., Gailus-Durner, V., et al., 2006. Generation and characterization of dickkopf3 mutant mice. Mol. Cell Biol. 26 (6), 2317–2326.
Destaing, O., Saltel, F., Gilquin, B., Chabadel, A., Khochbin, S., Ory, S., et al., 2005. A novel Rho-mDia2-HDAC6 pathway controls podosome patterning through microtubule acetylation in osteoclasts. J. Cell Sci. 118 (13), 2901–2911.
Fu, Y., Xu, Z., Wen, B., Gao, J., Chen, Z., 2020. Gonad-specific transcriptomes reveal differential expression of gene and miRNA between male and female of the discus fish (*Symphysodon aequifasciatus*). Front. Physiol. 11, 754.
Ghayor, C., Weber, F.E., 2016. Epigenetic regulation of bone remodeling and its impacts in osteoporosis. Int. J. Mol. Sci. 17 (9), 1446.
Glass II, D.A., Bialek, P., Ahn, J.D., Starbuck, M., Patel, M.S., Clevers, H., et al., 2005. Canonical Wnt signaling in differentiated osteoblasts controls osteoclast differentiation. Dev. Cell 8 (5), 751–764.
Godschalk, R., Remels, A., Hoogendoorn, C., van Benthem, J., Luijten, M., Duale, N., et al., 2018. Paternal exposure to environmental chemical stress affects male offspring's hepatic mitochondria. Toxicol. Sci. 162 (1), 241–250.
Godschalk, R.W., Verhofstad, N., Verheijen, M., Yauk, C.L., Linschooten, J.O., van Steeg, H., et al., 2015. Effects of benzo[*a*]pyrene on mouse germ cells: heritable DNA mutation, testicular cell hypomethylation and their interaction with nucleotide excision repair. Toxicol. Res. 4 (3), 718–724.
Grandjean, V., Gounon, P., Wagner, N., Martin, L., Wagner, K.D., Bernex, F., et al., 2009. The miR-124-Sox9 paramutation: rNA-mediated epigenetic control of embryonic and adult growth. Development 136 (21), 3647–3655.
Grün, D., Kester, L., Van Oudenaarden, A., 2014. Validation of noise models for single-cell transcriptomics. Nat. Methods 11 (6), 637.
Han, M., Xu, W., Cheng, P., Jin, H., Wang, X., 2017. Histone demethylase lysine demethylase 5B in development and cancer. Oncotarget 8 (5), 8980.
Hinoi, E., Fujimori, S., Wang, L., Hojo, H., Uno, K., Yoneda, Y., 2006. Nrf2 negatively regulates osteoblast differentiation via interfering with Runx2-dependent transcriptional activation. J. Biol. Chem. 281 (26), 18015–18024.
Hoshi, H., Hao, W., Fujita, Y., Funayama, A., Miyauchi, Y., Hashimoto, K., et al., 2012. Aldehyde-stress resulting from Aldh2 mutation promotes osteoporosis due to impaired osteoblastogenesis. J. Bone Miner. Res. 27 (9), 2015–2023.
Iqbal, J., Sun, L., Cao, J., Yuen, T., Lu, P., Bab, I., et al., 2013. Smoke carcinogens cause bone loss through the aryl hydrocarbon receptor and induction of Cyp1 enzymes. Proc. Natl. Acad. Sci. USA. 110 (27), 11115–11120.
Izawa, T., Arakaki, R., Mori, H., Tsunematsu, T., Kudo, Y., Tanaka, E., et al., 2016. The nuclear receptor AhR controls bone homeostasis by regulating osteoclast differentiation via the RANK/c-Fos signaling axis. J. Immunol. 197 (12), 4639–4650.
Jensen, E.D., Schroeder, T.M., Bailey, J., Gopalakrishnan, R., Westendorf, J.J., 2008. Histone deacetylase 7 associates with Runx2 and represses its activity during osteoblast maturation in a deacetylation-independent manner. J. Bone Miner. Res. 23 (3), 361–372.
Jin, Z., Wei, W., Dechow, P.C., Wan, Y., 2013. HDAC7 inhibits osteoclastogenesis by reversing RANKL-triggered β-catenin switch. Mol. Endocrinol. 27 (2), 325–335.
Jones, D.H., Kong, Y.Y., Penninger, J.M., 2002. Role of RANKL and RANK in bone loss and arthritis. Ann. Rheum. Dis. 61 (suppl 2), ii32–ii39 ii32-ii39.
Kim, K.M., Lim, S.K., 2014. Role of miRNAs in bone and their potential as therapeutic targets. Curr. Opin. Pharmacol. 16, 133–141.
Kobayashi, Y., Uehara, S., Udagawa, N., Takahashi, N., 2016. Regulation of bone metabolism by Wnt signals. J. Biochem. 159 (4), 387–392.
Kokabu, S., Gamer, L., Cox, K., Lowery, J., Tsuji, K., Raz, R., et al., 2012. BMP3 suppresses osteoblast differentiation of bone marrow stromal cells via interaction with Acvr2b. J. Mol. Endocrinol. 26 (1), 87–94.
Kong, R.Y.C., Giesy, J.P., Wu, R.S.S., Chen, E.X.H., Chiang, M.W.L., Lim, P.L., et al., 2008. Development of a marine fish model for studying in vivo molecular responses in ecotoxicology. Aquat. Toxicol. 86 (2), 131–141.
Langmead, B., 2010. Aligning short sequencing reads with Bowtie. Curr. Protoc. Bioinformatics 32 (1), 11–17.
Li, J.W., Lin, X., Tse, A., Cheung, A., Chan, T.F., Kong, R.Y.C., et al., 2016. Discovery and functional characterization of novel

miRNAs in the marine medaka *Oryzias melastigma*. Aquat. Toxicol. 175, 106–116.
Liao, Y., Smyth, G.K., Shi, W., 2014. featureCounts: an efficient general purpose program for assigning sequence reads to genomic features. Bioinformatics 30 (7), 923–930.
Ma, S., Wang, D.D., Ma, C.Y., Zhang, Y.D., 2019. microRNA-96 promotes osteoblast differentiation and bone formation in ankylosing spondylitis mice through activating the Wnt signaling pathway by binding to SOST. J. Cell Biochem. 120 (9), 15429–15442.
Mashiba, T., Turner, C.H., Hirano, T., Forwood, M.R., Jacob, D.S., Johnston, C.C., et al., 2001. Effects of high-dose etidronate treatment on microdamage accumulation and biomechanical properties in beagle bone before occurrence of spontaneous fractures. Bone 29 (3), 271–278.
McGee-Lawrence, M.E., Carpio, L.R., Schulze, R.J., Pierce, J.L., McNiven, M.A., Farr, J.N., et al., 2016. Hdac3 deficiency increases marrow adiposity and induces lipid storage and glucocorticoid metabolism in osteochondro progenitor cells. J. Bone Miner. Res. 31 (1), 116–128.
McPherson, N.O., Fullston, T., Aitken, R.J., Lane, M., 2014. Paternal obesity, interventions, and mechanistic pathways to impaired health in offspring. Ann. Nutr. Metab. 64 (3–4), 231–238.
Mlakar, S.J., Prezelj, J., Marc, J., 2012. Testing GSTP1 genotypes and haplotypes interactions in Slovenian post-/pre-menopausal women: novel involvement of glutathione S-transferases in bone remodeling process. Maturitas 71 (2), 180–187.
Mo, J., Au, D.W.T., Guo, J., Winkler, C., Kong, R.Y.C., Seemann, F., 2021. Benzo[a]pyrene osteotoxicity and the regulatory roles of genetic and epigenetic factors: a review. Crit. Rev. Environ. Sci. Technol. 1–39.
Mo, J., Au, D.W.T., Wan, M.T., Shi, J., Zhang, G., Winkler, C., et al., 2020. Multigenerational impacts of benzo[*a*]pyrene on bone modeling and remodeling in medaka (*Oryzias latipes*). Environ. Sci. Technol. 54 (19), 12271–12284.
Moffat, I., Chepelev, N.L., Labib, S., Bourdon-Lacombe, J., Kuo, B., Buick, J.K., et al., 2015. Comparison of toxicogenomics and traditional approaches to inform mode of action and points of departure in human health risk assessment of benzo[a]pyrene in drinking water. Crit. Rev. Toxicol. 45 (1), 1–43.
Ohtake, F., Baba, A., Takada, I., Okada, M., Iwasaki, K., Miki, H., et al., 2007. Dioxin receptor is a ligand-dependent E3 ubiquitin ligase. Nature 446 (7135), 562–566.
Omata, Y., Yasui, T., Hirose, J., Izawa, N., Imai, Y., Matsumoto, T., et al., 2015. Genomewide comprehensive analysis reveals critical cooperation between Smad and c-Fos in RANKL-induced osteoclastogenesis. J. Bone Miner. Res. 30 (5), 869–877.
Paine, R.T., Ruesink, J.L., Sun, A., Soulanille, E.L., Wonham, M.J., Harley, C.D., et al., 1996. Trouble on oiled waters: lessons from the Exxon Valdez oil spill. Annu. Rev. Ecol. Evol. Syst. 27 (1), 197–235.
Peterson, S.M., Thompson, J.A., Ufkin, M.L., Sathyanarayana, P., Liaw, L., Congdon, C.B., 2014. Common features of microRNA target prediction tools. Front. Genet. 5, 23.
Qiang, J., Tao, Y.F., He, J., Xu, P., Bao, J.W., Sun, Y.L., 2017. miR-122 promotes hepatic antioxidant defense of genetically improved farmed tilapia (GIFT, *Oreochromis niloticus*) exposed to cadmium by directly targeting a metallothionein gene. Aquat. Toxicol. 182, 39–48.
Qiang, Y.W., Chen, Y., Brown, N., Hu, B., Epstein, J., Barlogie, B., et al., 2010. Characterization of Wnt/β-catenin signalling in osteoclasts in multiple myeloma. Br. J. Haematol. 148 (5), 726–738.
Rando, O.J., 2016. Intergenerational transfer of epigenetic information in sperm. Cold spring harb. Perspect. Med. 6 (5), a022988.
Rassoulzadegan, M., Grandjean, V., Gounon, P., Vincent, S., Gillot, I., Cuzin, F., 2006. RNA-mediated non-mendelian inheritance of an epigenetic change in the mouse. Nature 441 (7092), 469–474.
Renn, J., Büttner, A., To, T.T., Chan, S.J.H., Winkler, C., 2013. A *col10a1*: nlGFP transgenic line displays putative osteoblast precursors at the medaka notochordal sheath prior to mineralization. Dev. Biol. 381 (1), 134–143.
Schneider, A.J., Branam, A.M., Peterson, R.E., 2014. Intersection of AHR and Wnt signaling in development, health, and disease. Int. J. Mol Sci. 15 (10), 17852–17885.
Seemann, F., Jeong, C.B., Zhang, G., Wan, M.T., Guo, B., Peterson, D.R., et al., 2017. Ancestral benzo[a]pyrene exposure affects bone integrity in F3 adult fish (*Oryzias latipes*). Aquat. Toxicol. 183, 127–134.
Seemann, F., Peterson, D.R., Witten, P.E., Guo, B.S., Shanthanagouda, A.H., Ye, R.R., et al., 2015. Insight into the transgenerational effect of benzo[*a*]pyrene on bone formation in a teleost fish (*Oryzias latipes*). Comp. Biochem. Physiol. C Toxicol. Pharmacol. 178, 60–67.
Skinner, M.K., 2008. What is an epigenetic transgenerational phenotype? F3 or F2. Reprod. Toxicol. 25 (1), 2–6.
Shanthanagouda, A.H., Guo, B.S., Ye, R.R., Chao, L., Chiang, M.W., Singaram, G., et al., 2014. Japanese medaka: a non-mammalian vertebrate model for studying sex and age-related bone metabolism in vivo. PLoS One 9 (2), e88165.
Sun, Y.X., Li, L., Corry, K.A., Zhang, P., Yang, Y., Himes, E., et al., 2015. Deletion of Nrf2 reduces skeletal mechanical properties and decreases load-driven bone formation. Bone 74, 1–9.
Tong, Y., Niu, M., Du, Y., Mei, W., Cao, W., Dou, Y., et al., 2017. Aryl hydrocarbon receptor suppresses the osteogenesis of mesenchymal stem cells in collagen-induced arthritic mice through the inhibition of β-catenin. Exp. Cell Res. 350 (2), 349–357.
Van Kesteren, P.C.E., Zwart, P.E., Schaap, M.M., Pronk, T.E., van Herwijnen, M.H.M., Kleinjans, J.C.S., et al., 2013. Benzo[*a*]pyrene-induced transcriptomic responses in primary hepatocytes and in vivo liver: toxicokinetics is essential for *in vivo–in vitro* comparisons. Arch. Toxicol. 87 (3), 505–515.
Vanhees, K., Vonhögen, I.G., van Schooten, F.J., Godschalk, R.W., 2014. You are what you eat, and so are your children: the impact of micronutrients on the epigenetic programming of offspring. Cell. Mol. Life Sci. 71 (2), 271–285.
Wagner, K.D., Wagner, N., Ghanbarian, H., Grandjean, V., Gounon, P., Cuzin, F., et al., 2008. RNA induction and inheritance of epigenetic cardiac hypertrophy in the mouse. Dev. Cell 14 (6), 962–969.
Wang, Y., Li, Y.P., Paulson, C., Shao, J.Z., Zhang, X., Wu, M., et al., 2014. Wnt and the Wnt signaling pathway in bone development and disease. Ront. Biosci. 19, 379.
Westendorf, J.J., Zaidi, S.K., Cascino, J.E., Kahler, R., Van Wijnen, A.J., Lian, J.B., et al., 2002. Runx2 (Cbfa1, AML-3) interacts with histone deacetylase 6 and represses the p21CIP1/WAF1 promoter. Mol. Cell Biol. 22 (22), 7982–7992.
Xu, E.G., Mager, E.M., Grosell, M., Pasparakis, C., Schlenker, L.S., Stieglitz, J.D., et al., 2016. Time-and oil-dependent transcriptomic and physiological responses to Deepwater Horizon oil in mahi-mahi (*Coryphaena hippurus*) embryos and larvae. Environ. Sci. Technol. 50 (14), 7842–7851.
Yu, H., Jiang, L., Wan, B., Zhang, W., Yao, L., Che, T., et al., 2018. The role of aryl hydrocarbon receptor in bone remodeling. Prog. Biophys. Mol. Biol. 134, 44–49.
Yu, T., Witten, P.E., Huysseune, A., Buettner, A., To, T.T., Winkler, C., 2016. Live imaging of osteoclast inhibition by bisphosphonates in a medaka osteoporosis model. Dis. Model Mech. 9 (2), 155–163.

Yu, T.Y., Pang, W.J., Yang, G.S., 2015. Aryl hydrocarbon receptors in osteoclast lineage cells are a negative regulator of bone mass. PLoS One 10 (1), e0117112.
Zhang, W., Liu, Y., Yu, H., Du, X., Zhang, Q., Wang, X., et al., 2016. Transcriptome analysis of the gonads of olive flounder (*Paralichthys olivaceus*). Fish Physiol. Biochem. 42 (6), 1581–1594.
Zheng, H., Liu, J., Tycksen, E., Nunley, R., McAlinden, A., 2019. MicroRNA-181a/b-1 over-expression enhances osteogenesis by modulating PTEN/PI3K/AKT signaling and mitochondrial metabolism. Bone 123, 92–102.
Zhou, L., Qiu, M., Yang, L., Yang, L., Zhang, Y., Mu, S., et al., 2020. MicroRNA-1-3p enhances osteoblast differentiation of MC3T3-E1 cells by interacting with hypoxia-inducible factor 1 α inhibitor (HIF1AN). Mech. Dev., 103613.